Supporting Information

Mixed-ion strategy to construct CNTs-decorated Co/N-doped hollow carbon for enhanced oxygen reduction

Taotao Feng[a] *and Meining Zhang**[a]

Department of Chemistry, Renmin University of China, Beijing 100872, P. R. China

*E-mail: mnzhang@ruc.edu.cn

Experimental

Reagent and solution. Tetraethyl silicate (TEOS, 28.4%), Methanol (CH_3OH), Cobaltous sulfate heptahydrate ($CoSO_4 \cdot 7H_2O$) were obtained from Sinopharm Chemical Reagent Co., Ltd. Ethanol (CH_3CH_2OH), Hydrofluoric acid (HF), Hydrochloric acid (HCl), Sulfuric acid (H_2SO_4), Zinc sulfate heptahydrate ($ZnSO_4 \cdot 7H_2O$) and Sodium hydroxide (NaOH) were purchased from Beijing Chemical Works. Ammonium hydroxide ($NH_3 \cdot H_2O$, Beijing Modern oriental Fine Chemistry Co., Ltd), 2-methylimidazole (2-MeIm, 98%, Adamas Reagent Co., Ltd), Potassium hydroxide (KOH, Aladdin Reagent), nafion solution (5 wt%, Shanghai Hesen Electric Appliance Co., Ltd) and Pt catalysts (Pt/XC-72, 20 wt%, Alfa Aesar) were purchased.

Preparation of SiO_2. SiO_2 was prepared using a modified stöber method. Typically, 11.2 mL of TEOS was added into 112 mL of ethanol/deionized solution, then adding 20 mL of $NH_3 \cdot H_2O$ into above solution. Followed the above solution was stirred for 2 h. The SiO_2 were centrifuged, and washed with ethanol three times and dried at 60°C for 12 h.

Preparation of SiO_2@ZIFs-Co_xZn_{1-x}. a mol of $CoSO_4 \cdot 7H_2O$ and 12.3-a mol of $ZnSO_4 \cdot 7H_2O$ (a = 0, 0.65, 2.84, 9.23, 11.07, and 12.3 mol), and 8.22 g of 2-MeIm were dissolved into 120 mL and 200 mL of methanol, respectively. Then, the 120 mL of mixed solution was immediately added into the 2-MeIm solution. 10 mL of SiO_2 solution (1 $mg \cdot mL^{-1}$) was added into the above solution with magnetic stirring, and the mixtures were further stirring for 3 h. Finally, the purple solid product was collected by centrifugation and washed with methanol. After drying at 60°C for overnight, the as-prepared a series of core-shell SiO_2@ZIF-Co_xZn_{1-x} were obtained.

Preparation of CNTs decorated on Co/N-Doped Hollow Carbon hybrids (CNTs-Co/NHC-x). The as-prepared core-shell SiO_2@ZIF-Co_xZn_{1-x} product was pyrolyzed at a definite temperature (900°C) for 3 h under Ar atmosphere (constant flow of 40 sccm). The obtained powder was processed in HF solution (5 wt%) and 2 M HCl solution for 12 h, respectively, and washed thoroughly with deionized ethanol and water. After drying at 80°C for 12 h, a series of CNTs decorated on Co/N-Doped Hollow Carbon (CNTs-Co/NHC-x) hybrids was obtained.

Preparation of Co/N-Doped Hollow Carbon hybrids (Co/NHC). In contrast, the both as-prepared core-shell SiO_2@ZIF-Co and SiO_2@ZIF-Zn product also was pyrolyzed under above same definite temperature (900°C) for 3 h under Ar atmosphere. Then, the obtained powder was processed in HF solution (5 wt%) and 2 M HCl solution for 12 h, respectively, and washed thoroughly with deionized ethanol and water. After drying at 80°C for 12 h, the Co/N-Doped Hollow Carbon hybrids (Co/NHC) and N-Doped Hollow Carbon hybrids (NHC) was obtained, respectively.

Characterization. SEM measurements were carried out on a HITACHI SU8010 scanning electron microscope. XRD measurements was carried out on a SHIMADZU XRD-7000 diffractomer. Raman spectrum analyses was recorded on an XploRA™ PLUS Raman spectrometer. Thermogravimetric (TGA) analysis was performed on a TA instruments Q500 (TA Instruments New Castle, DE) under N_2. FT-IR was performed with a SHIMADZU IR Prestige-21 FT-IR spectrometer. XPS were recorded on a Thermos ESCALAB 250. The nitrogen sorption isotherms were measured by using BelSorp-Mini II automatic volumetric adsorption equipment, and Barrett-Emmett-Teller (BET) surface area were calculated by using the Barrett-Joyner-Halenda (BJH) method. TEM and HRTEM were taken on a JEOL JEM-2100F field-emission high-resolution transmission electron microscope.

Electrochemical Text. All electrochemical measurements were performed on an electrochemical workstation (CHI 760D, Shanghai, China) in a conventional three-electrode electrochemical cell, with a electrocatalyst modified glass carbon electrode (GCE) (diameter, 3 mm) or rotating ring disk electrode (RRDE) (diameter, 4 mm) as working electrode, a platinum wire as the auxiliary electrode and a saturated Ag/AgCl (saturated with 3 M KCl) as reference electrode. The catalyst ink was prepared by adding 2 mg of catalyst (or commercial Pt/C, 20 wt%) into 1 mL of mixed solution containing ethanol and 5.0 wt% Nafion at a volume ratio of 39:1 under ultrasonic agitation to form a homogeneous catalyst suspension (2 mg·mL^{-1}). Then, a calculated amount (6.3 μL) of commercial Pt/C catalyst ink was evenly cast on the surface of pre-cleaned RRDE, and dried at room temperature, corresponding to 0.1 mg·cm^{-2} of commercial Pt/C. Likewise, the non-precious metal catalyst modified pre-cleaned GCE or RRDE surface also obtained, and the loadings were 0.2 mg·cm^{-2}. Before test, an Ar or O_2 flow was used for the electrolyte in cell for 30 min to give a saturation state. CV curves were recorded in Ar- or O_2-saturated 0.1 M KOH solution with a scan rate of 20 mV·s^{-1}. LSV curves were recorded in O_2-saturated 0.1 M KOH solution containing 0.2 M KCl at different speed rates (400, 625, 900, 1225 and 1600 rpm) with a scan rate of 20 mV·s^{-1}. The disk potential was cycled from -1.0 to 0.2 V (vs. Ag/AgCl) at a scan rate of 20 mV·s^{-1}. A flow of O_2 was maintained over the electrolyte during the LSV test to ensure O_2 saturation. All the current density in this work was calculated based on the geometrical area of glass carbon electrode or rotating disk electrode.

We calculated the number of electron transfer (n) and the H_2O_2 percent yield (wt%) involved in ORR using the following equations:

$$n = \frac{4I_d}{\left(I_d + \frac{I_r}{N}\right)}$$

$$H_2O_2(\%) = \frac{200I_r}{N \times I_d + I_r}$$

Where I_d and I_r are the disk current and the ring current, respectively, and N is the current collection efficiency of Pt ring and was determined to be 0.42.

For investigation of the possible reasons for the excellent ORR activity of CNTs-Co/NHC-x catalyst, it is necessary to explore the electrocatalytic mechanisms and the reaction kinetics of CNTs-Co/NHC-x catalyst toward ORR. The ORR performance of CNTs-Co/NHC-x catalyst in the kinetic-limiting and diffusion-limiting region can be investigated using the Koutecky-Levich (K-L) equations:

$$\frac{1}{J} = \frac{1}{J_L} + \frac{1}{J_K} = \frac{1}{B\omega^{\frac{1}{2}}} + \frac{1}{J_K}$$

$$B = 0.62nFC_0\left(D_0\right)^{\frac{2}{3}} \nu^{-\frac{1}{6}}$$

Where J is the measured current density, J_K and J_L are the kinetic-limiting and diffusion-limiting current densities, ω is the angular frequency of the rotation in terms of rad·s^{-1}, n is transferred electron number during ORR, F is the Faraday constant (96485 C·mol^{-1}), C_0 is the bulk concentration of oxygen (1.2×10^{-6} mol·cm^{-3} for 0.1 M KOH), D_0 is the diffusion coefficient of oxygen in the electrolyte, and v is the kinematic viscosity of the electrolyte.

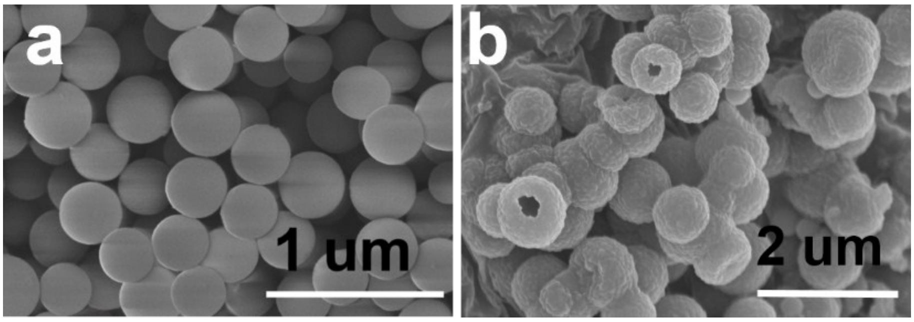

Fig. S1 SEM image of (a) SiO_2 and (b) core-shell SiO_2@ZIFs-Co precursor (Namely, x = 1 in the SiO_2@ZIFs-Co_xZn_{1-x} precursor).

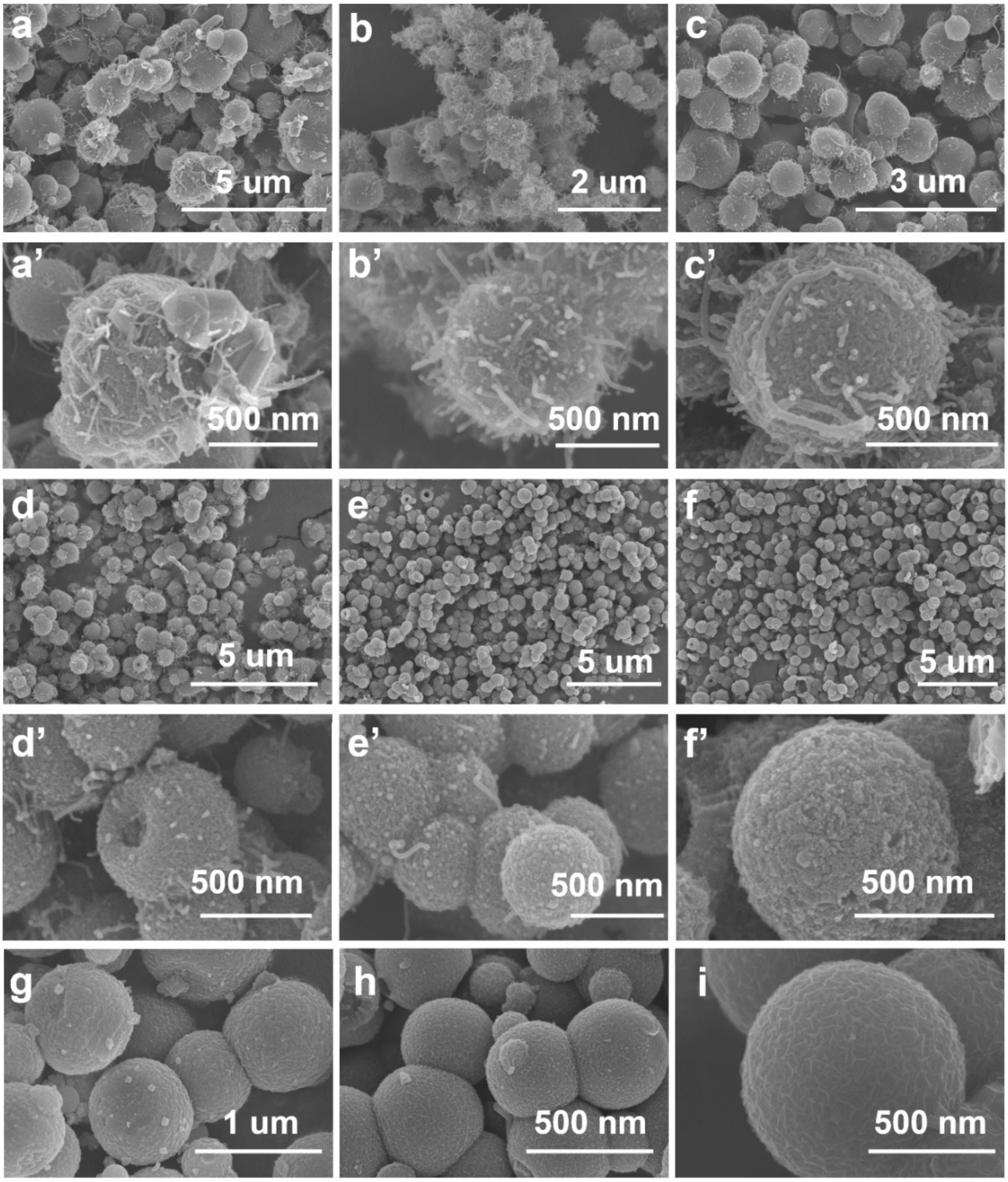

Fig. S2 SEM image of different content CNTs structure anchored on Co/NHC hybrids derived from SiO_2@ZIFs-Co_xZn_{1-x} precursor [x = 0.09 (a, a’), 0.23 (b, b’), 0.5 (c, c’), 0.75 (d, d’), 0.90 (e, e’) and 1 (f, f’)]. SEM image of SiO_2@ZIF-Co_0Zn_1 (g) its pyrolysis product (h, i) without CNTs on the carbon surface.

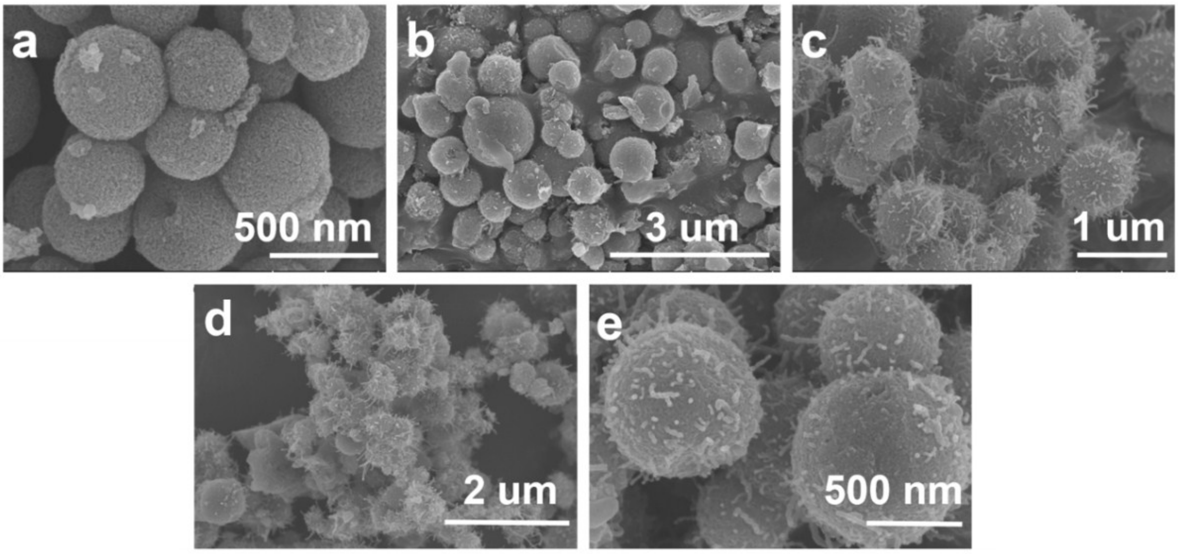

Fig. S3 SEM image of different content CNTs structure anchored on Co/NHC hybrids derived from SiO_2@ZIFs-$Co_{0.23}Zn_{0.77}$ precursor at different temperature [600 ºC (a), 700 ºC (b), 800 ºC (c), 900 ºC (d), 1000 ºC (e)].

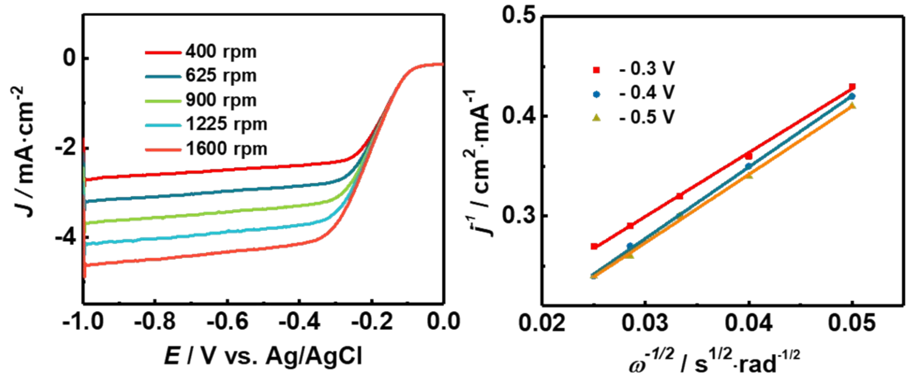

Figure S4. (a) RDE voltammograms of electrode modified with Co/NHC at different rotation rates from 400 to 1600 rpm. (b) the corresponding Koutecky-Levich plots for the Co/NHC electrocatalysts at -0.3 ~ -0.5 V (vs. Ag/AgCl).

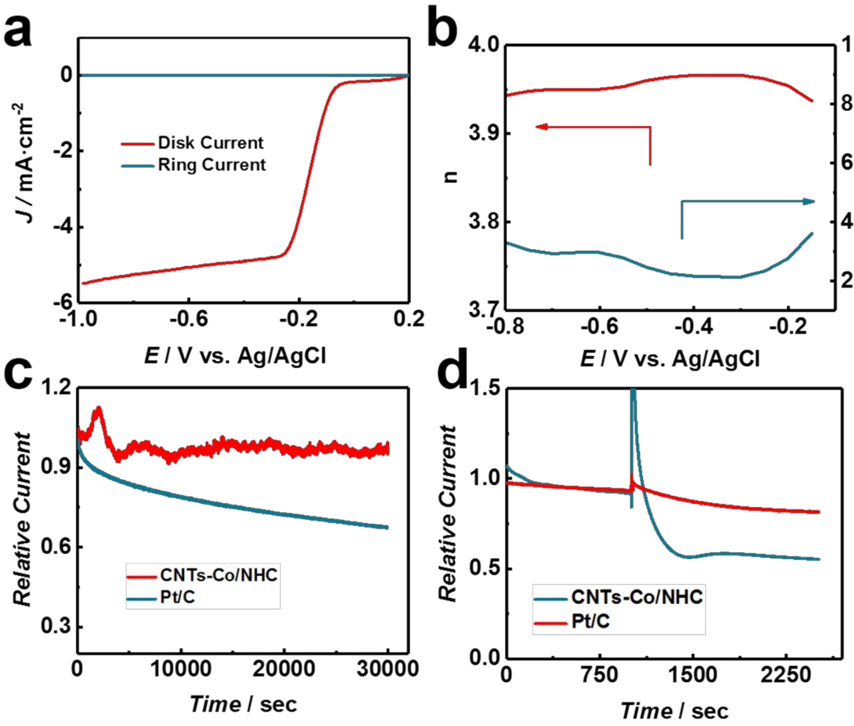

Fig. S5 (a) RRDE of modified electrode with CNTs-Co/NHC-0.23 in O_2-saturated 0.1 M KOH solution at a rotational speed of 1600 rpm. (b) the electron transferred number (*n*) and H_2O_2 yield during ORR calculated from RRDE. (c) Chronoamperometry test in O_2-saturated 0.1M KOH solution at -0.3 V (vs. Ag/AgCl) on electrode modified with CNTs-Co/NHC-0.23 and Pt/C for 30000 s. (f) Chronoamperometric responses on electrode modified with CNTs-Co/NHC-0.23 and Pt/C on addition of 2.0 M methanol after about 1000 s.

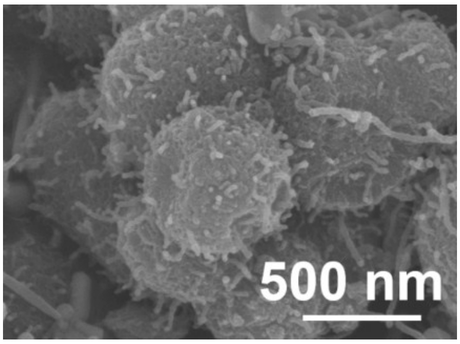

Fig. S6 SEM images of CNTs-Co/NHC after electrochemical test.

Table S1. Comparison of the catalytic activity of nitrogen-doped carbon for ORR.

Sample	E_{onset} (V vs. RHE)	$E_{1/2}$ (V vs. RHE)	n	Ref.
Co@N-CNTs-m	0.929	0.849	3.5~3.8	S1
Co-MOF@CNTs	0.91	0.82	3.7	S2
Co-C@NWCs	0.939	0.83	3.99	S3
NCNCs	-0.15	-0.26	3.27	S4
NT-G	0.89	0.76	—	S5
NOMGAs	-0.15 (vs. Ag/AgCl)	-0.28 (vs. Ag/AgCl)	3.9	S6
NDMC	-0.02	-0.13	3.2	S7
CoO@N/S-CNF	0.84	0.722	4.00	S8
MnCoO-NCNTs	—	—	3.8	S9
CNT/HDC	0.92	0.82	—	S10
CNTs-Co/NHC-0.23	-0.03 V (vs. Ag/AgCl) 0.95 V	-0.15 V (vs. Ag/AgCl) 0.84 V	3.96	Our work

note#

Co@N-CNTs-m: Cobalt nanoparticle-encapsulated nitrogen-doped carbon nanotubes.

Co-C@NWCs: nitrogen-enriched core-shell structured cobalt-carbon nanoparticles sequentially aligned on wrinkles of nitrogen-doped carbon nanosheets.

NCNCs: Nitrogen-doped carbon nanocages.

NT-G: few-walled (two to three walls) carbon nanotube-graphene hybrid.

NOMGAs: nitrogen-doped ordered mesoporous graphitic arrays.

NDMC: Nitrogen-doped mesoporous carbon.

CoO@N/S-CNF: CoO embedding nanoparticles into nitrogen and sulfur co-doped carbon nanofiber networks.

MnCoO-NCNTs: spinel Mn-Co oxide nanoparticles partially embedded in N-doped carbon nanotubes.

CNT/HDC: carbon nanotubes/heteroatom-doped carbon.

Supplementary references

(1) S. L. Zhang, Y. Zhang, W. J. Jiang, X. Liu, S. L. Xu, R. J. Huo, F. Z. Zhang, J. S. Hu, Carbon 2016, 107, 162-170.

(2) Y. Fang, X. Li, F. Li, X. Lin, M. Tian, X. Long, X. An, Y. Fu, J. Jin, J. Ma, J. Power Sources 2016, 326, 50-59.

(3) Y. Li, F. Cheng, J. Zhang, Z. Chen, Q. Xu, S. Guo, Small 2016, 12, 2839-2845.

(4) S. Chen, J. Bi, Y. Zhao, L. Yang, C. Zhang, Y. Ma, Q. Wu, X. Wang, Z. Hu, Adv. Mater. 2012, 24, 5593.

(5) Y. Li, W. Zhou, H. Wang, L. Xie, Y. Liang, F. Wei, J. C. Idrobo, S. J. Pennycook, H. Dai, Nature Nanotechnology, 2012, 7, 394-400.

(6) R. Liu, D. Wu, X. Feng, K. Müllen, Angew. Chem. Int. Ed. 2010, 49, 2565.

(7) W. Yang, T. P. Fellinger, M. J. Antonietti, J. Am. Chem. Soc. 2011, 133, 206.

(8) T. Liu, Y. F. Guo, Y. M. Yan, F. Wang, C. Deng, D. Rooney, K. N. Sun, Carbon 2016, 106, 84-92.

(9) A. Zhao, J. Masa, W. Xia, A. Maljusch, M. G. Willinger, G. Clavel, K. Xie, R. Schlogl, W. Schuhmann, M. Muhler, J. Am. Chem. Soc. 2014, 136, 7551-7554.

(10) Y. J. Sa, C. Park, H. Y. Jeong, S. H. Park, Z. Lee, K. T. Kim, G. G. Park, S. H. Joo, Angew. Chem. Int. Ed. 2014, 53, 4102.